Study on Poly(ethylene terephthalate)/Polypropylene Microfibrillar Composites. II. Solid-State Drawing Behavior

X. D. Lin,[1] D. Jia,[1] F. K. P. Leung,[2] W. L. Cheung[2]

[1]*Department of Polymer Materials Science and Engineering, South China University of Technology, Guangzhou, China*
[2]*Department of Mechanical Engineering, The University of Hong Kong, Hong Kong, China*

Received 10 July 2003; accepted 18 February 2004
DOI 10.1002/app.20618
Published online in Wiley InterScience (www.interscience.wiley.com).

ABSTRACT: A (20/80) blend of poly(ethylene terephthalate)/polypropylene (PET/PP) was solid-state drawn to enhance the molecular orientation of the PET microfibers. Effects of drawing temperature (23–140°C) and drawing speed (max. 1000 mm/min) on the morphology and draw ratio of the blend were studied and discussed based on the drawing behaviors of the pure polymers. In cold drawing, there seemed to be a critical drawing speed below which the natural draw ratios of the polymers remained constant, but above which the draw ratios first decreased slightly because of suppression of molecular relaxation and then increased because of breakage of highly strained molecules and disintegration of lamellar crystals into finer mosaic blocks. Macroscopically, the pure PP and the PET/PP composite extrudates gave similar draw ratios at the same speeds. SEM showed that the PET microfibers suffered a smaller elongation than the PP matrix and severe voiding occurred at the PET/PP interface. Furthermore, substantial fiber breakage occurred during cold drawing at speeds above 200 mm/min. In comparison, drawing at 100°C caused no obvious interfacial voiding and fiber breakage. Furthermore, the natural draw ratio of the blend was lower than that of the pure PP extrudate, indicating that the PET microfibers had constrained the deformation of the PP matrix. © 2004 Wiley Periodicals, Inc. J Appl Polym Sci 93: 1989–2000, 2004

Key words: blends; drawing; morphology; extrusion; molecular dynamics

INTRODUCTION

Solid-state forming has long been used to improve the mechanical properties of metals. In the last three decades, it has also been adopted for processing polymers.[1] One important objective is to achieve a high molecular orientation with the express aim of improving the mechanical properties. As the name suggests, solid-state forming should take place below the melting temperature (T_m) of crystalline polymers or softening temperature (T_s) of amorphous polymers. Because materials exhibit a brittle behavior below the glass-transition temperature (T_g) and few examples of solid-state forming are possible, solid-state forming is thus normally performed between T_g and T_m or T_s. There is no distinct temperature boundary between solid-state forming and thermoforming. Usually, solid-state forming takes place at a lower temperature than that of thermoforming.[2]

Ordinary cold drawing likely causes voiding in the drawn material and results in whitening. On the other hand, high-temperature drawing does not give a high molecular orientation. Zone drawing and zone annealing provide a possible solution to the above two undesirable phenomena.[3] It provides energy for entangled molecules to relax and slip; otherwise, they will break and result in fracture of the drawn parts. This enables those still disoriented molecules to align along the drawing direction. As a result, the sample can be drawn to a higher draw ratio. Also, annealing causes crystallization, which helps to fix the orientation achieved. The process was adopted for producing microfibrillar composites.[4,5] Two-stage drawing, which consists of tensile drawing first at a lower temperature then at a higher temperature, was also used to achieve a higher deformation ratio (>10) and thus a higher strength.[6,7]

In our previous article,[8] the morphological development of a PET/PP (20/80) microfibrillar composite in melt extrusion was reported. Because the PET microfibers in the extrudates were formed in a molten state and under a moderate hauling speed (15 m/min), the degree of molecular orientation was expected to be similar to that of randomly oriented PET. In this work, solid-state drawing was performed on the PET/PP

Correspondence to: W. L. Cheung.
Contract grant sponsor: Competitive Earmarked Research Grant (CERG) of Hong Kong Research Grants Council; contract grant number: HKU 7064/00E.

composite extrudates at different speeds and temperatures to increase the molecular orientation and strength of the reinforcing PET microfibers in the blend. The morphologies of the composite PET/PP extrudates after drawing at different temperatures were examined by scanning electron microscopy (SEM). Some PET microfibers were extracted from the blend by xylene and subsequently examined by SEM. The effects of drawing speed and drawing temperature on the natural draw ratio of the composite extrudates were studied and discussed based on the drawing behaviors of the pure polymers and the concept of a polymer network.

EXPERIMENTAL

Solid-state drawing

The isotactic PP resin used was Shell VM6100 and the PET resin was Arnite D04 300; the extrusion process was reported earlier.[8] Solid-state drawing of the PET, PP, and PET/PP (20/80) extrudates was performed on a Lloyd tensile tester (JJ Lloyd Instruments, Hampshire, UK) at room temperature (~ 23°C), 60, 100, and 140°C. For drawing at above room temperature, the extrudates were conditioned in the thermal chamber for 30 min before drawing. The distance between the grips was 10 mm. Different drawing speeds, ranging from 2 to 1000 mm/min, were used. When the drawing process was completed, the drawn extrudates were quenched to room temperature by immediately opening the door of the thermal chamber. Drawing of low-crystallinity PET at 100°C produced a uniform deformation of the gauge length and therefore the draw ratio could be deliberately controlled by setting different extension limits. The draw ratios were determined by measuring the separations between the ink marks on the gauge length before and after drawing.

Extraction of PET microfibers

The PET microfibers were extracted from both the as-extruded and solid-state drawn PET/PP extrudates by dissolving the PP matrix in a heated xylene solution. The extrudates were first wrapped in perforated aluminum foil and then submerged in xylene contained in a flask with a water-cooling reflux column. For each extraction step, the xylene was heated to a boil (~ 138°C) for 3 h and then allowed to cool at ambient conditions. After cooling, the PP precipitates and gelled material were filtered out and some fresh xylene was added to the flask to compensate for the loss of xylene. Two extraction steps were performed each day and the overall extraction process lasted for 1 week.

Measurement of elastic moduli of PET, PP, and PET/PP extrudates

The elastic moduli of the extrudates were measured using a DMTA IV dynamic mechanical thermal analyzer (Rheometric Scientific, Piscataway, NJ). The diameters of the extrudates were calculated based on their weight, length, and density data. A tensile mode at 1 Hz was used for the tests. The temperature was raised from room temperature to 160°C at a rate of 3°C/min.

Differential scanning calorimetry

The thermal behavior of the PET extrudate before and after solid-state drawing was investigated using a Dupont (Boston, MA) 910 differential scanning calorimeter. The scan rate was 10°C/min. A flow of nitrogen, 20 mL/min, was used as the purging gas. The degrees of crystallinity of the as-extruded and drawn PET samples were determined based on the cold crystallization exotherm and the melting endotherm. The enthalpy of melting of crystalline PET was taken as 140 J/g.[9]

Scanning electron microscopy

The morphologies of the PET/PP extrudates before and after solid-state drawing were studied. The samples were split after being dipped into liquid nitrogen. The fracture surfaces were then sputtered with gold–palladium. A Cambridge S440 scanning electron microscope (Cambridge, UK) was used for the examination.

RESULTS AND DISCUSSION

Drawing behavior of PP

When drawn at room temperature, the PP extrudates exhibited a distinctive yield point followed by necking and cold drawing. The deformation mechanisms and reorientation of the lamellar crystals during cold drawing of semicrystalline polymers have been studied extensively. There are imperfect lattice fits (mosaic boundaries) between the coherent mosaic blocks. During cold drawing, the crystals tend to fail along the mosaic boundaries and then break into folded chain blocks that in turn serve as building elements of the new polymer network structure.[10,11] If the test is stopped in the constant-load region of the load–extension curve, the drawn region or the neck of the specimen will suffer an extension corresponding to the natural draw ratio. Figure 1 shows the plot of natural draw ratio of the extrudates against drawing speed. It can be divided into three regions: I (drawing speed < 10 mm/min) is a region of constant draw ratio; II (drawing speed between 10 and 50 mm/min) is a transition region within which the draw ratio drops

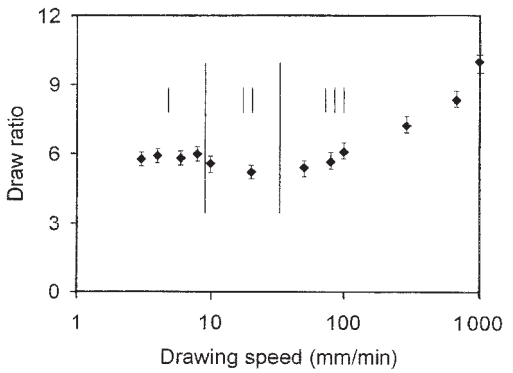

Figure 1 Effect of drawing speed on draw ratio of PP extrudates at 23°C.

slightly; and III (drawing speed > 50 mm/min) is a region within which the draw ratio increases with drawing speed.

Polymers are viscoelastic materials. When the strain rate is low, as in region I, relaxation of the tort molecules can occur and the drawing stress is low. Very few of the entangled molecules will break and lamellar crystals fail only along the weak mosaic boundaries and the nature draw ratio is more or less constant. On the other hand, when the strain rate is high, as in region III, relaxation is prohibited and the molecular entanglements within the polymer network become locked (the phenomenon is called "strain rate lock" hereafter). Under this condition, a higher stress is generated within the polymer network, which can cause breakage of some highly strained molecules and lamellar crystals to split at locations where they do not normally split under a low drawing stress. Because the crystals form a major part of the entanglement points in semicrystalline polymers, this effectively increases the size of the polymer network, thus giving rise to an increase in the natural draw ratio. The drawing speed should exceed a certain critical value for strain rate lock to operate and it should correspond to the relaxation behavior of the strained molecules within the network. In this case, the critical drawing speed is probably between 10 and 50 mm/min (i.e., region II of Fig. 1). Within this region, the amount of slippage at some entanglement points would decrease because of strain rate lock. However, the drawing stress was not high enough to cause substantial breakage of the entangled molecules and disintegration of the lamellar crystals. As a result, the natural draw ratio decreased slightly.

Figure 2 shows the relations between the natural draw ratio and drawing speed at 60 and 100°C. The natural draw ratio remains generally constant at 5.5 (for 60°C) and 6 (for 100°C), up to 1000 mm/min, and it is similar to that of the samples cold drawn at speeds below 10 mm/min (i.e., before strain rate lock). The phenomenon can be attributed to the fact that the drawing temperatures were well above the T_g (−10°C) of PP; therefore, relaxation of the amorphous molecules was facilitated and the entanglement points of the polymer network were primarily associated with the crystals, the properties of which are generally independent of temperature below the melting point. Furthermore, the results suggest that, if molecular relaxation is allowed during drawing (e.g., during cold drawing at low speed or drawing at moderate temperatures), the network structure does not change significantly. The above results are in agreement with those of Long and Ward[12] and Radhakrishnan and Gupta,[13] obtained in a state of flow drawing. It is expected that for high-temperature drawing, strain rate lock can operate only at very high drawing speeds. However, the facility did not allow drawing experiments at speeds above 1000 mm/min to be performed.

The network structure of a semicrystalline polymer is dependent on the density of entanglement points and which can be divided into two categories: (1) molecular entanglements in the amorphous material and (2) crystals. Low-speed drawing facilitates relaxation of (1). There should be a number of stable category (1) entanglements that are dependent on molecular weight and temperature. For a totally amorphous polymer, the number will decrease significantly at above the softening temperature and the material behaves like a viscous fluid. In a semicrystalline polymer, category (2) entanglements should be dependent on the degree of crystallinity and crystal structure but generally independent of temperature below the melting point. Because PP has a substantially high degree of crystallinity (~ 60%), it is believed that the majority of the entanglements of the network structure are of category (2) in nature. This explains why the change of temperature had little effect on the natural draw ratio.

Drawing behavior of PET

During cold drawing at speeds below 50 mm/min, the PET extrudates exhibited a distinctive yield point followed by necking and smooth growth of the neck. The

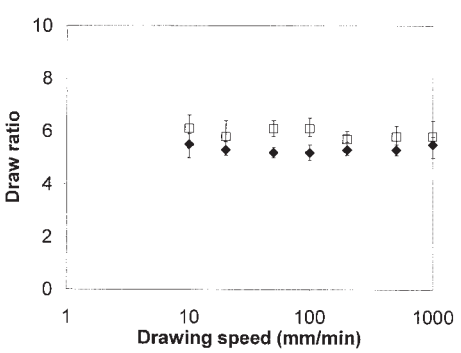

Figure 2 Effect of drawing speed on the natural draw ratio of PP extrudates at 60°C (◆) and 100°C (□).

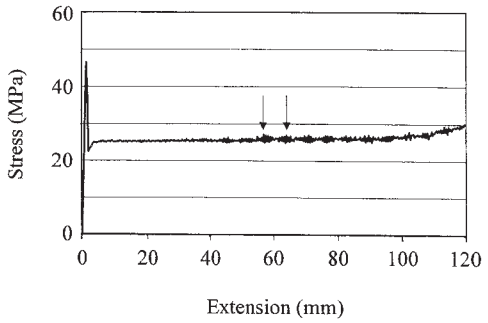

Figure 3 Stress–extension curve of PET extrudate during cold drawing at 400 mm/min. Arrows show fluctuation of the drawing stress during self-oscillated neck propagation.

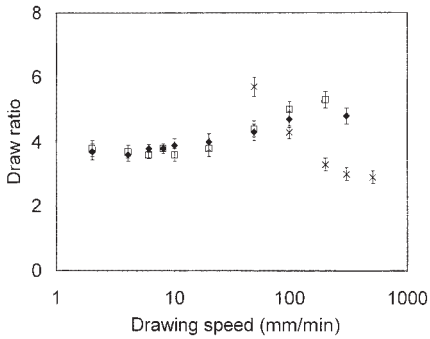

Figure 5 Effect of drawing speed on the natural draw ratio of PET extrudates at 23°C (□), 60°C (◆), and 100°C (×).

material in the neck remained generally transparent after drawing. When the drawing speed exceeded 50 mm/min, however, spontaneous oscillation of neck growth occurred near the end of the drawing process, and there was a corresponding fluctuation of the drawing stress (Fig. 3). The phenomenon produced alternating sections of transparent and whitened material, as shown in Figure 4. Self-oscillated neck propagation was attributed to intensive local heating.[14] As drawing continues, elastic deformation of the drawn portion becomes large. When the aggregated elastic deformation or energy has reached a certain level, it will be released very quickly by drawing the undrawn parts at a speed much faster than the drawing speed provided by the tensile machine. Then, the undrawn parts stop being drawn and elastic deformation begins to aggregate again for another cycle of oscillation. Generally, self-oscillation takes place only after the neck has grown to a certain length and a higher drawing speed will initiate the phenomenon earlier.

Figure 5 shows the natural draw ratio of PET under different drawing conditions. For cold drawing and drawing at 60°C, there was little change in the natural draw ratio at drawing speeds below 10 mm/min. Above 10 mm/min, however, the draw ratio increased with increasing drawing speed. In general, the trend was similar to cold drawing of the PP extrudates.

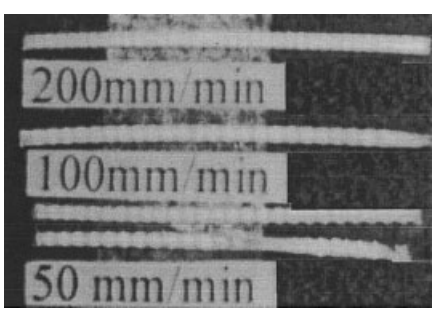

Figure 4 Self-oscillated neck of PET extrudates after cold drawing.

However, the rate of increase in the natural draw ratio was lower at 60°C than at room temperature. This can be attributed to the fact that the higher drawing temperature facilitated relaxation of the entangled molecules and reduced the drawing stress. This in turn lowered the extent of disintegration of the lamellar crystals and breakage of the entangled molecules. In other words, the increase in network size was less significant for drawing at 60°C than at room temperature under the same drawing speed.

Figure 6 shows the DSC thermographs of the undrawn extrudate and extrudates cold drawn at different speeds. Typically, the undrawn extrudate [curve (a)] had a distinctive T_g at about 80°C, which was followed by a sharp crystallization peak at about 130°C and a melting peak at 253°C. Based on the crystallization exotherm and the fusion endotherm, and taking the enthalpy of melting of crystalline PET as 140 J/g,[9] the crystallinity of the undrawn extrudate was calculated to be about 10%. After cold drawing, however, the crystallization peak reduced to a broad hump, covering a temperature range from the glass transition to the original crystallization peak of the undrawn extrudate, and the originally downward trend of the DSC thermograph at T_g became more or less horizontal. The phenomena can be attributed to drawing-induced crystallization, which partially consumed the crystallizable material and orientated other amorphous molecules in a more favorable position for crystallization. During the subsequent DSC scan, crystallization started at a lower temperature near the glass-transition temperature, thus changing the shape of the DSC thermograph. As the drawing speed was increased, drawing-induced crystallization became more complete. This depleted the amount of material for crystallization during the subsequent DSC analysis and therefore the hump became flatter. In the case of after drawing at 200 mm/min, both the glass-transition temperature and crystallization peak were hardly noticeable.

Furthermore, the melting peak of the cold-drawn extrudates became sharper. Nicholas et al.[15] used the maximum melting peak height as an indirect measure

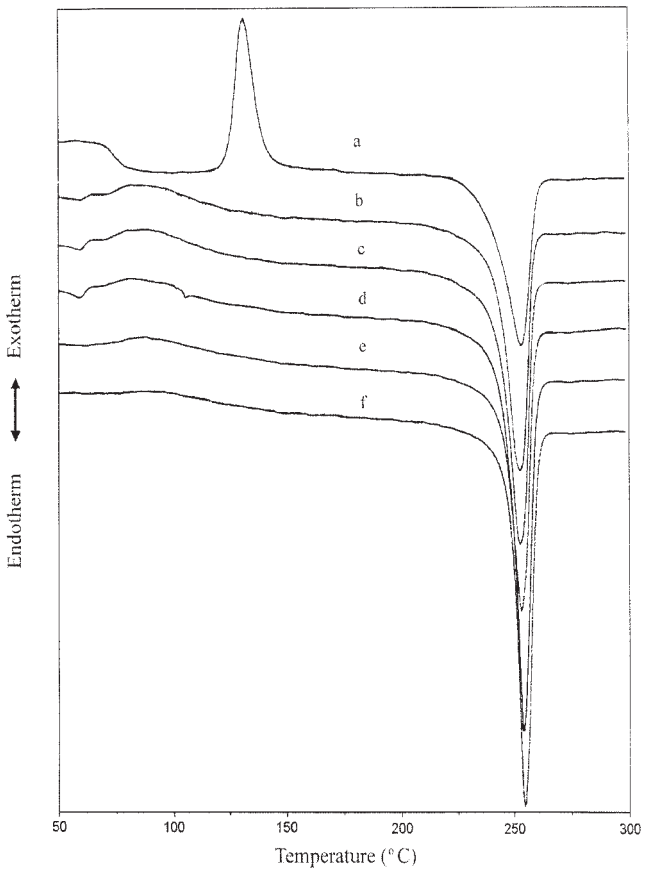

Figure 6 DSC thermographs of PET extrudates: (a) before solid-state drawing, and after cold drawing at (b) 10 mm/min; (c) 20 mm/min; (d) 50 mm/min; (e) 100 mm/min; and (f) 200 mm/min.

of the molecular orientation in drawn PET and found an approximately linear relation between it and Herman's function. The relative melting peak height (R) (i.e., ratio of the fusion peak height of a drawn extrudate to that of the undrawn extrudate) and other fusion parameters of our drawn PET extrudates were determined and are listed in Table I. R was found to increase with drawing speed and draw ratio. There was an upward shift of the onset temperature of melting after drawing. It is well known that the breadth of the melting peak is a consequence of the lower order of perfection of polymer crystallites. The results suggested that the proportion of the less-perfect crystallites had decreased with increasing draw ratio.

In contrast to cold drawing, drawing at 100°C gave quite a different load–extension behavior. No clear necking of the specimen was observed and the deformation was generally uniform along the whole gauge length. The specimens after drawing remained more or less transparent. At low drawing speeds (<50 mm/min), the drawing stress remained generally constant up to the extension limit provided by the tensile machine. The phenomenon can be attributed to flow drawing of the polymer. It has been reported that drawing at low velocity of amorphous and low-crystallinity PET at 100°C gives no orientation. This is because crystal sites are not large and dense enough to provide effective links between molecules, and thus simple molecular entanglements lose effect because the relaxation time is short. Under this condition, molecular relaxation processes predominate over the orientation process. The polymer molecules may slip past one another and flow individually, exhibiting a large deformation without inducing any molecular orientation and crystallization.[16,17]

At higher drawing speeds, however, the load increased when the drawing process had proceeded through a certain distance (Fig. 7). This was attributed to strain-induced crystallization[18,19] and the density of entanglement points had increased significantly. Figure 8 shows some overlaid DSC thermographs of the PET extrudates drawn at 200 mm/min to different draw ratios (obtained by stopping the tests at different elongations). The crystallization peak decreased and shifted to a lower temperature with increasing draw ratio. A similar phenomenon was observed in a study on PET films biaxially stretched at 100°C.[20] As the draw ratio was increased from 1 to 5.8, the crystallization endotherm decreased from 25.2 to 1.2 J/g because of depletion of the crystallizable material resulting from strain-induced crystallization. Figure 9 shows the relations between the relative melting peak height (R) and the draw ratio for both the cold-drawn samples and samples drawn at 100°C. A generally linear relation was obtained for the 100°C drawn samples. For the cold-drawn sam-

TABLE I
Draw Ratio and Fusion Parameters of PET Extrudates After Cold Drawing at Different Speeds

Parameter	Drawing speed (mm/min)					
	Undrawn	10	20	50	100	200
Draw ratio	1	3.6	3.8	4.4	5.0	5.3
Fusion heat (J/g)	39.6	49.4	51.1	50.7	50.9	52.2
Onset temperature (°C)	238.8	242.0	242.9	243.9	248.3	249.7
Melting temperature (°C)	253.2	253.1	252.8	253.4	254.6	254.8
R	1	1.44	1.60	1.69	2.13	2.27

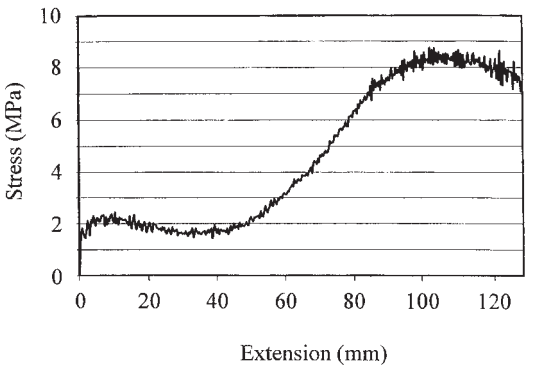

Figure 7 Stress–extension curve of PET extrudate drawn at 100°C and 400 mm/min, showing strain hardening above an extension of 40 mm.

ples, no data were obtained for $\lambda < 3.5$ because of nonhomogeneous deformation during the drawing process. For $\lambda \geq 3.6$, however, the relative melting peak height of the cold-drawn samples increased more steeply than that of the 100°C drawn samples. This is likely attributable to the different relaxation behaviors at the drawing temperatures.

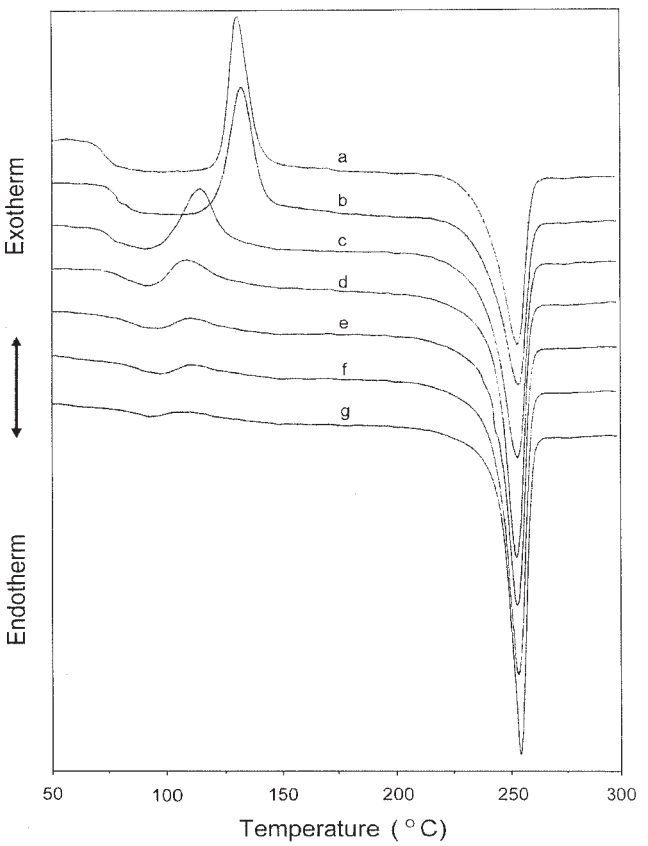

Figure 8 DSC thermographs of (a) undrawn PET extrudate and extrudates drawn at 100°C and 200 mm/min to different draw ratios: (b) $\lambda = 1.2$; (c) $\lambda = 2.5$; (d) $\lambda = 3.0$; (e) $\lambda = 3.5$; (f) $\lambda = 4.6$; and (g) $\lambda = 5.8$.

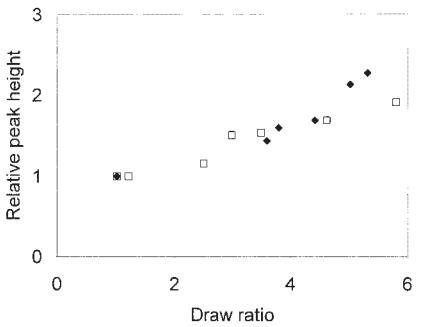

Figure 9 Relative melting peak height as a function of draw ratio for PET extrudates after cold drawing (◆) and drawing at 100°C (□).

Figure 10 shows the change of crystallinity of the PET extrudates after drawing to different ratios (λ). No significant changes were observed below $\lambda = 1.7$. In fact, there is a critical draw ratio, about 1.5 to 1.6, for strain-induced crystallization to take place.[18] The same draw ratio holds true even for roll drawing.[21] Furthermore, the critical draw ratio for strain-induced crystallization is dependent on strain rate: the lower the strain rate, the higher the critical draw ratio.[22] The kinetics of crystallization during stretching is controlled by the evolution of orientation of the amorphous molecules and so the rate of crystallization increases with strain rate.[23] On the other hand, a higher drawing temperature delays the beginning of crystallization because of a lower amorphous orientation in the material. Between λ values of 1.7 and 3.5, the crystallinity increased significantly from about 10 to 34%, and a further increase in λ caused only a slight further increase in the crystallinity.

For drawing at 100°C, it was not possible to determine the natural draw ratio at drawing speeds below 50 mm/min because of flow drawing. However, strain-induced crystallization occurred at 50 mm/min and above, and the drawing load showed an obvious increasing trend after a certain elongation. It was noted that the minimum drawing speed to cause

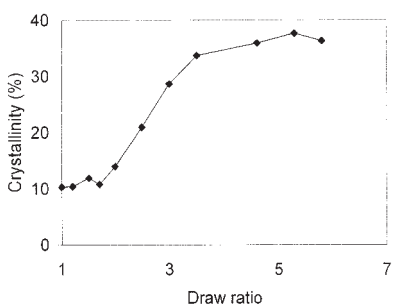

Figure 10 Effect of draw ratio on degree of crystallinity of PET extrudates. Drawing temperature: 100°C; drawing speed: 200 mm/min.

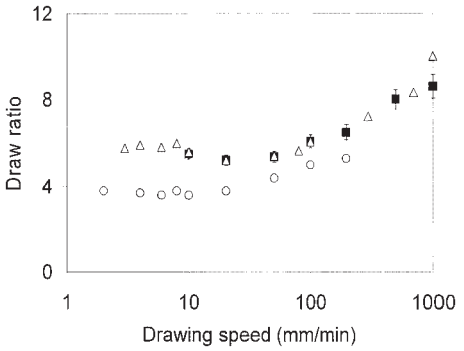

Figure 11 Effect of drawing speed on the natural draw ratio of PET/PP extrudates (■). Draw ratios of pure PP extrudates (△) and pure PET extrudates (○) are included for comparison. Drawing temperature: 23°C.

strain-induced crystallization was affected by the initial crystallinity of the extrudate. In another experiment with PET extrudates of lower initial crystallinity (~ 6%), strain-induced crystallization did not occur until the drawing speed was above 200 mm/min. To investigate the effect of drawing speed on natural draw ratio, the tests were stopped when the increasing trend of the load was clearly established and the draw ratio at the point of inflection of the load–extension curve was taken as the natural draw ratio.[13] It can be seen from Figure 5 that the natural draw ratio decreases relatively rapidly from 5.7 at 50 mm/min to about 3.3 at 200 mm/min and then levels off at about 3 for drawing speeds above 300 mm/min. It is also noteworthy that from Figure 10, the corresponding crystallinity at the natural draw ratio for 200 mm/min coincides with the beginning of the upper plateau region (i.e., ~ 30%). Because the natural draw ratio for 100°C drawing was evaluated based on the inflection point of the load–extension curve, it can thus be concluded that strain hardening becomes apparent only when the crystallinity has reached a substantially high level. It has been reported that crystallinity below 25% does not significantly alter the network structure or density of entanglement points of PET.[24] In this experiment, the required draw ratio to attain the 25% critical crystallinity is about 3, which roughly coincides with the natural draw ratio.

Drawing behavior of PET/PP

Figure 11 shows a combined plot of the average draw ratios of the pure PP, pure PET, and PET/PP extrudates at room temperature. Basically, the draw ratio-versus drawing speed relation of the PET/PP composite extrudates was similar to that of the pure PP extrudates. In other words, the PET microfibers had little effect on the draw ratio of the blend. Figure 12 shows the longitudinal views of the PET/PP extrudates before and after drawing at different temperatures. The extrudates were cryogenically split and the fracture surfaces were approximately halfway between the skin and the center where both PET fibers and particles were abundant. The morphological details of the extrudate before drawing were discussed previously.[8] After cold drawing, whitening was observed in the

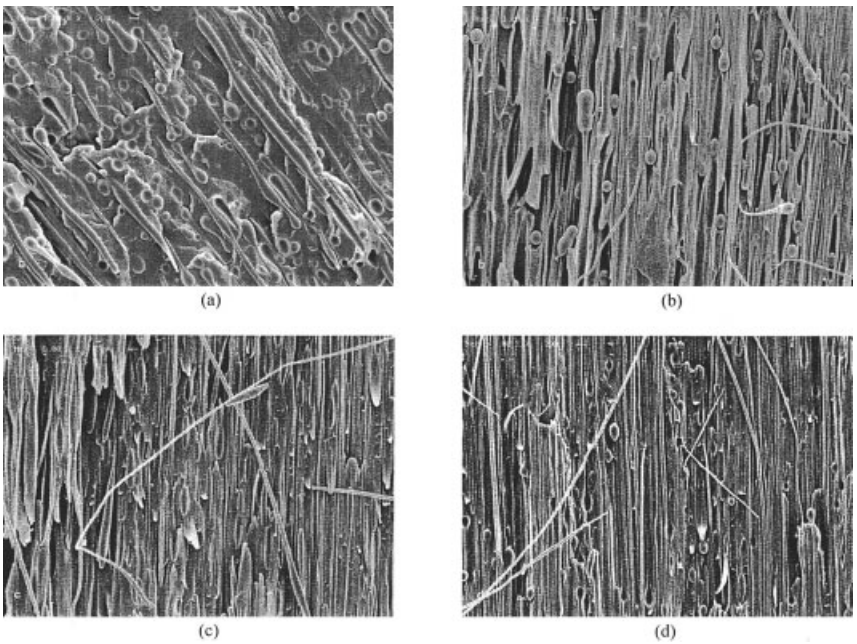

Figure 12 Morphology of PET/PP extrudates before solid-state drawing (a), and after solid-state drawing at 23°C (b), 100°C (c), and 140°C (d). Drawing speed: 100 mm/min.

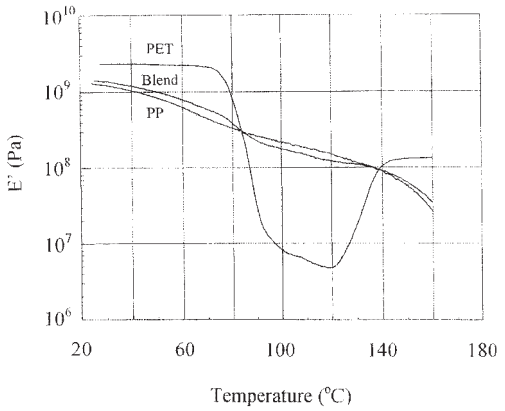

Figure 13 Dynamic mechanical analysis of PET, PP, and PET/PP extrudates. Testing mode: tensile; frequency: 1 Hz; heating rate: 3°C/min.

drawn section of the extrudate. Under SEM [Fig. 12(b)] the PET fibers suffered an extensive elongation in the midsection, whereas the fiber ends were generally undeformed. The PET fibers were debonded from the PP matrix and severe voiding occurred around the drawn sections of the fibers and beyond the fiber ends. This is explained by the fact that PP has a higher natural draw ratio than that of PET at room temperature and that the PET/PP interface is weak because of the incompatibility of the two polymers. Similar to the fiber ends, the spherical PET particles were generally undeformed. Once they were debonded, drawing was not possible because of the absence of tensile stress across the interface. Meanwhile, drawing of the PET fibers was still possibly attributable to friction on the circumferential surfaces of the unnecked regions and the enlarged fiber ends. The actual draw ratios of the PET microfibers within the composite extrudates could not be determined; nevertheless, they should be close to those of the pure PET extrudates drawn under similar speeds.

Figure 12(c) shows the longitudinal section of the blend after drawing at 100°C. Slight whitening was observed in the drawn section but it was less severe compared with that of the cold-drawn samples. No spherical PET particles were observed and all of them were deformed to ellipsoids with a relatively large a/b ratio. No severe voiding was observed at the interface and both the PET fibers and PP matrix suffered almost the same elongation. This was attributed to the high drawing temperature ($> T_g$) and the polymer was in a rubbery state. Because the modulus of PET falls below that of PP between 85 and 140°C (Fig. 13), the PET domains would thus change to whatever shape corresponded to the deformation of the PP matrix at low drawing speed. At high drawing speed, however, strain-induced crystallization and strain hardening of the PET domains will occur; as a result, the PET domains may restrain the deformation of the PP matrix at a later stage of the drawing process. Figure 12(d) shows the composite extrudate drawn at 140°C. Although most PET domains were drawn to slender fibers, some spherical PET particles were still present. This can be attributed to the increased modulus resulting from crystallization during annealing at such high temperature.

Figure 14 shows the effect of drawing speed on the natural draw ratio of the blend at 100°C. The composite extrudate exhibited a lower draw ratio than that of the pure PP extrudate within the range of drawing speeds. This suggests that the PET microfibers restrained the deformation of the PP matrix. It is surprising that this phenomenon holds true, even at drawing speeds below 20 mm/min, where the pure PET extrudate was undergoing a flow drawing process. Perhaps, the drawing behavior of the PET extrudate did not truly represent the drawing behavior of the PET microfibers within the blend. Although the extrusion parameters used for both the blend and the pure PET extrudate were the same, it was possible that the PET microfibers had a higher degree of molecular alignment or crystallinity than that of the PET extrudate. In this case, the PET microfibers might exhibit a lower natural draw ratio than that of the PP matrix, even at low drawing speed. Given that the draw ratio of PET microfibers was more or less the same as that of the blend, the microfibers suffered a noticeably higher draw ratio than the natural draw ratio of the pure PET extrudate at high drawing speeds. This is advantageous in terms of enhancing the molecular alignment within the microfibers.

Figure 15 shows the PET fibers extracted from the as-extruded PET/PP blend. The diameters of the PET fibers were roughly 1 μm and varied along the length. The wavy morphology was a result of capillary instability of the elongated PET domains during the melt-extrusion process.[25] Most fibers have enlarged round ends. The designation "A" denotes a fiber end that is about to break away from the main body of the fiber

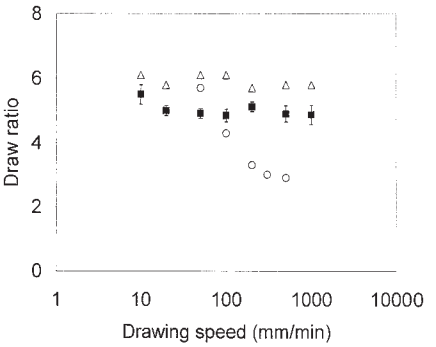

Figure 14 Effect of drawing speed on the natural draw ratio of PET/PP extrudates (■). Average draw ratios of pure PP extrudates (△) and pure PET extrudates (○) are shown for comparison. Drawing temperature: 100°C.

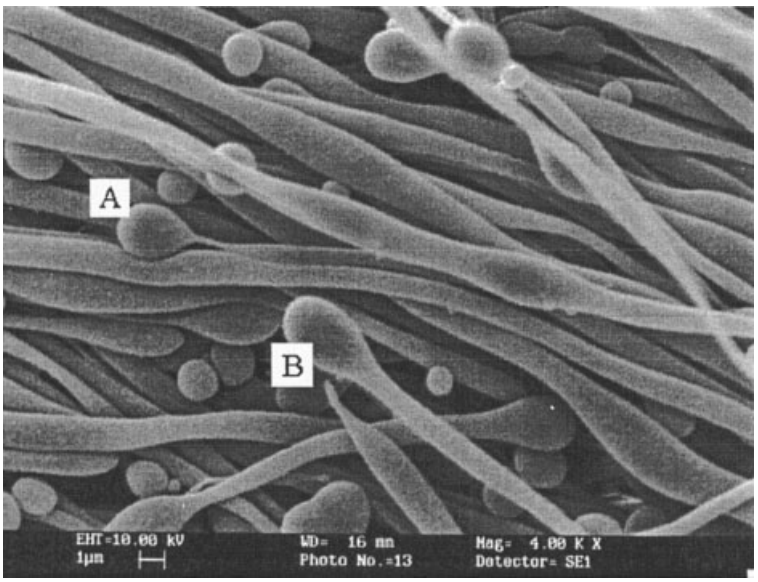

Figure 15 PET fibers extracted from the as-extruded blend.

and "B" denotes a pointed fiber end from which the enlarged round end has just broken off. Figure 16 shows the PET fibers extracted from the PET/PP extrudate after cold drawing at 1000 mm/min. The midsections of the PET fibers became more slender and most of them were about 0.5 μm in diameter. The helical morphology was ascribed to nonuniform shrinkage of the cold-drawn PET fibers during extraction.[26] Cold drawing of the pure PET extrudates at speeds higher than 200 mm/min was scarcely feasible. On the other hand, the composite PET/PP extrudates could be cold drawn at much faster speeds to produce PET microfibers within the PP matrix. However, some of the PET fibers were broken into small fragments, as shown in Figure 17. The sharp ends of these fragments indicate a brittle failure of the fibers.

Figure 18 shows the PET fibers extracted from a PET/PP extrudate drawn at 100°C and 200 mm/min. The helical morphology of the fibers indicates the presence of residual stresses, even though drawing was performed at above the T_g of the polymer. As described in Figure 12(c), no spherical PET particles were found after drawing. The formerly round fiber ends became highly elongated. In addition, no obvious fiber breakage was observed, even up to a drawing speed of 1000 mm/min. For drawing at 140°C (Fig.

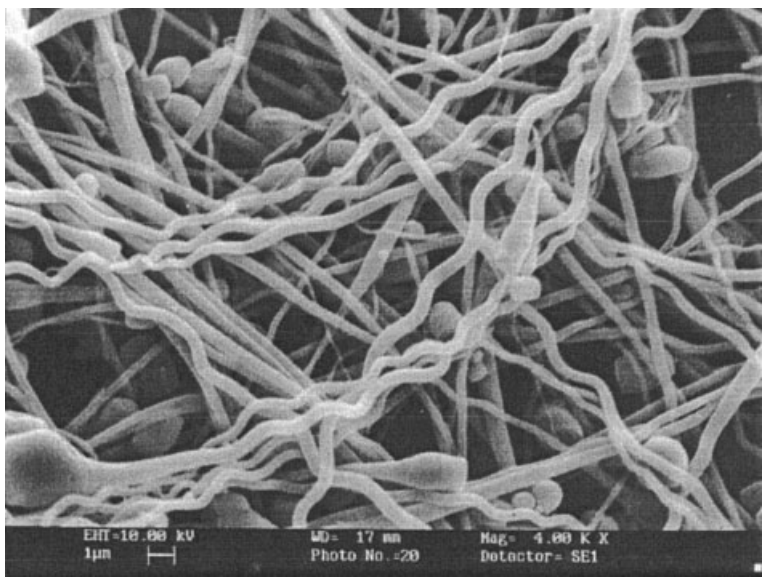

Figure 16 PET fibers extracted from cold-drawn PET/PP extrudates. Drawing speed: 1000 mm/min.

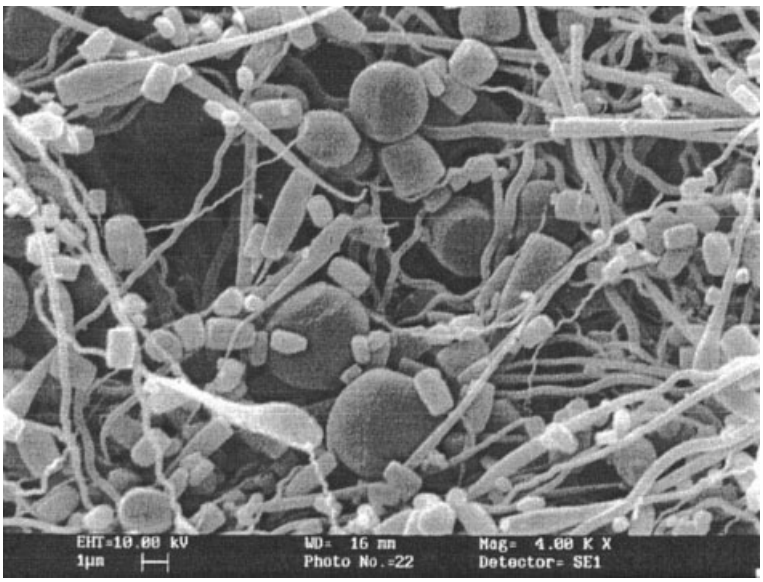

Figure 17 Broken fragments of PET fibers extracted from a PET/PP extrudate after cold drawing at 1000 mm/min. Sharp fracture surfaces indicate brittle failure of the fibers.

19) the extracted fibers were generally straight. This was probably attributable to relaxation and crystallization of the fibers during drawing at such high temperature, and the subsequent extraction process had little effect on the shrinkage of the fibers. Compared with Figure 18, the ends of the fibers drawn at 140°C were less elongated. As discussed before, this was ascribed to crystallization and hardening of the PET fibers during the thermal conditioning process before drawing.

CONCLUSIONS

In cold drawing, the PP extrudate had a constant natural draw ratio (~ 6) below 10 mm/min. When the drawing speed was above 10 mm/min, strain rate lock started to operate and there was a slight decrease of the natural draw ratio between 10 and 50 mm/min. Above 50 mm/min, the natural draw ratio increased with increasing drawing speed and this could be explained by enlargement of the polymer network that resulted from breakage of some entangled molecules and disintegration of lamellar crystals into finer mosaic blocks. At 60 and 100°C, the natural draw ratio of PP remained generally constant between 5.5 and 6 over the whole range of drawing speeds. The phenomenon was attributed to relaxation of the amorphous molecules under the drawing conditions and the entanglement points of the polymer network were primarily associated with the crystals.

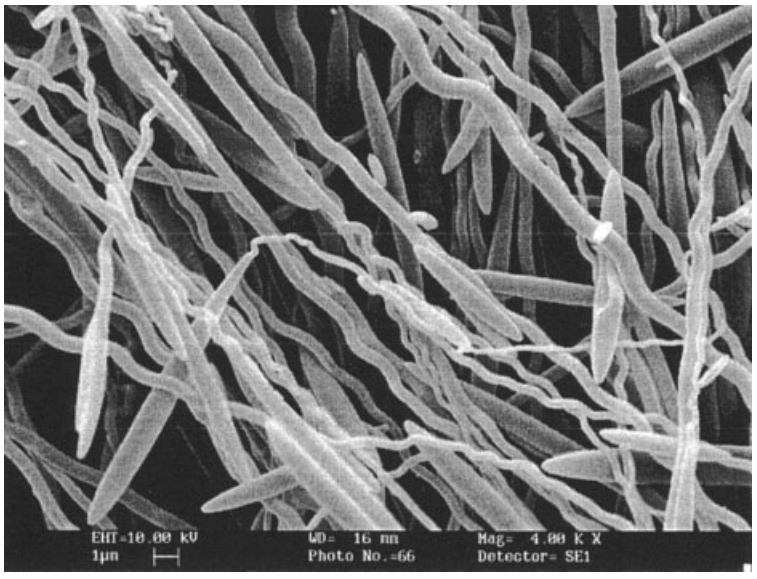

Figure 18 PET fibers extracted from a PET/PP extrudate drawn at 100°C and 200 mm/min.

Figure 19 PET fibers extracted from a PET/PP extrudate drawn at 140°C and 200 mm/min.

The drawing behavior of the PET extrudate at room temperature and 60°C exhibited a similar trend as the cold drawing behavior of the PP, except that the PET had a lower natural draw ratio under the same drawing speed. Nevertheless, the rate of increase in the natural draw ratio after the critical drawing speed was lower at 60°C than at room temperature. This could be explained by the slightly higher mobility of the entangled molecules, which favored molecular relaxation rather than strain rate lock; therefore, enlargement of the polymer network resulting from breakage of entangled molecules and disintegration of crystals was suppressed.

At 100°C, flow drawing of PET occurred below 50 mm/min. The extrudate exhibited a natural draw ratio at drawing speeds only above 50 mm/min because of strain hardening. The natural draw ratio first decreased rapidly and then leveled off at about 3 for drawing speeds faster than 200 mm/min. At 200 mm/min, strain-induced crystallization was not obvious below a draw ratio of 1.7, which can be considered as the critical draw ratio for strain-induced crystallization under the drawing condition. Further drawing between λ values of 1.7 and 3.5 caused the crystallinity to increase sharply from 10 to 35%. The natural draw ratio was found to be associated with the crystallinity development of the samples. Apparently, strain hardening occurred when the crystallinity had reached about 30% because of a significant increase in the density of entanglement points in the polymer network, which in turn limited the flow of the molecules.

Because PET has a smaller draw ratio than that of PP at low temperature and the PET/PP interface is weak, cold drawing of the PET/PP extrudates led to severe debonding of the PET fibers and particles. Consequently, the natural draw ratio of the composite extrudates was similar to that of the PP extrudates. In addition, drawing at speeds above 200 mm/min led to substantial breakage of the PET microfibers. Drawing at 100°C, on the other hand, showed no obvious sign of interfacial debonding. The composite extrudate had a lower natural draw ratio than that of the PP extrudate, indicating that the PET microfibers inhibited the deformation of the PP matrix.

This project was supported by a Competitive Earmarked Research Grant (CERG) of the Hong Kong Research Grants Council (Project Code HKU 7064/00E).

References

1. Ward, I. M. Plast Rubber Compos Process Appl 1993, 19, 7.
2. Jungnickel, B. J.; Käufer, H.; Leyrer, K. H.; Mennig, G.; Wendorff, J. H. In Solid State Forming of Polymers; Bartz, W. J., Ed.; Mechanical Engineering Publications: London, 1992; Chapter 1.
3. Kunugi, T.; Suzuki, A.; Akiyama, I.; Hashimoto, M. Polym Prepr (Am Chem Soc Div Polym Chem) 1979, 20, 778.
4. Evstatiev, M.; Fakirov, S. Polymer 1992, 33, 877.
5. Fakirov, S.; Evstatiev, M.; Schultz, J. M. Polymer 1993, 34, 4669.
6. AKZO N.V. (The Netherlands). Brit. Pat. 1,559,056 (1977).
7. Ito, M.; Miya, H.; Watanabe, M.; Kanamoto, T. J Appl Polym Sci 1990, 40, 543.
8. Lin, X.; Cheung, W. L. J Appl Polym Sci 2003, 88, 3100.
9. Wunderlich, B. Polym Eng Sci 1978, 18, 431.
10. Peterlin, A. J Mater Sci 1971, 6, 490.
11. Young, R. J.; Bowden, P. B.; Rider, J. G. J Mater Sci 1973, 8, 23.
12. Long, S. D.; Ward, I. M. J Appl Polym Sci 1991 42, 1911.
13. Radhakrishnan, J.; Gupta, V. B. J Macromol Sci Phys 1993, B32, 243.

14. Andrianova, G. P.; Kargin, V. A.; Kechekjan, A. S. J Polym Sci Part A-2 1971, 9, 1919.
15. Nicholas, P.; Lane, A. R.; Carter, T. J.; Hay, J. N. Polymer 1988, 29, 894.
16. Sasano, H.; Kawai, T. Makromol Chem 1983, 184, 217.
17. Gupta, V. B.; Sett, S. K.; Venkataraman, A. Polym Eng Sci 1990, 30, 1252.
18. Koenig, J. L.; Mele, M. D. Makromol Chem 1968, 118, 128.
19. Bechev, Chr.; Godovsky, Y. J Mater Sci 1982, 17, 817.
20. Cakmak, M.; White, J. L.; Spruiell, J. E. J Polym Eng 1986, 6, 291.
21. Matthew, R.; Ajji, A.; Cole, K. C.; Dumoulin, M. M. ANTEC'98, 1615.
22. Hermanutz, F.; Salem, D. R.; Wesson, S. P. Polymer 1994, 35, 4611.
23. Le Bourvellec, G.; Monnerie, L.; Jarry, J. P. Polymer 1987, 28, 1712.
24. Cansfield, D. L. M.; Patel, R.; Ward, I. M. J Macromol Sci Phys 1993, B32, 373.
25. Tomotika, S. Proc R Soc London 1935, 150, 322.
26. Spreeuwers, H. R.; van der Pol, G. M. W. Plast Rubber Compos Process Appl 1989, 11, 159.